A Noninvasive Method for Determining Dielectric Properties of Layered Tissues on Human Back

Article *in* Journal of Electromagnetic Waves and Applications · October 2007

DOI: 10.1163/156939307781890978

Liping Yan
Sichuan University

Changjun Liu
Sichuan University

J. of Electromagn. Waves and Appl., Vol. 21, No. 13, 1829–1843, 2007

A NONINVASIVE METHOD FOR DETERMINING DIELECTRIC PROPERTIES OF LAYERED TISSUES ON HUMAN BACK

L. P. Yan, K. M. Huang, and C. J. Liu

College of Electronics and Information Engineering
Sichuan University
Chengdu 610064, China

Abstract—A 3-dimensional (3D) reconstruction method based on layered-homogenous-tissue model to obtain dielectric properties of superficial tissues of human body by noninvasive measurement is presented in this paper. First a circle patch probe fed by coaxial line is optimized by using micro genetic algorithm (MGA) to measure reflection coefficient at a wide frequency range from 1 GHz to 7 GHz. Then reconstruction method based on MGA is discussed and verified by some experiments. Finally, the dielectric properties of skin, fat and muscle, as well as thickness of skin and fat, on the human back are reconstructed. The reconstructed results agree to the published data.

1. INTRODUCTION

Measurements indicate that relative dielectric constant and conductivity of high-water-content tissues are about an order of magnitude greater than those of low-water-content tissues. Moreover, the dielectric constant and conductivity of tumors are quite different from those of normal tissues [1–3]. That makes different tissues and especially abnormal tissues detection by using electromagnetic means possible.

Up to now there are mainly two electromagnetic methods which can provide the permittivity or conductivity of tissues. One takes advantage of very high frequency electromagnetic wave (EMW), such as microwave imaging (MI), the other takes advantage of low frequency EMW, such as electrical impedance tomography (EIT). Microwave imaging can provide not only permittivity images with high resolution, but also the images of temperature [4, 5]. Especially, a method of microwave imaging via space-time (MIST) beamforming make it possible to detect very small malignant tumors embedded within the complex fibroglandular structure of the breast [6]. EIT provide the conductivity distribution in tissues, whereas the resolution of the image is not high enough to detect the accurate electrical properties of very thin tissues, such as skin [7].

Both methods use either multi antennas or electrodes, which make the measurement system complex. A noninvasive method for determining the conductivity of a tissue layer embedded in stratified biological structure using only open-ended coaxial probe is presented by K. Huang [8]. However that open-ended probe only operates at 200 MHz.

Based on the method presented by K. Huang, a 3-dimensional (3D) reconstruction strategy using layered-homogenous-tissue model to get dielectric properties (dielectric constant and conductivity) of layered tissues on human back is presented in this paper. The stratified model, which consists of three layers, skin, fat and muscle, can quite well represent most of the body region [9]. And the complex tissue of each layer can be regarded as homogenous one in the case of physically small probe.

Different from the open-ended probe used in Huang's method, a patch antenna probe is presented and optimized by using micro genetic algorithm (MGA) combined with finite difference time domain (FDTD) method to measure reflection coefficient at a wide frequency range. Then the optimized probe is used in the measurement of human back. Finally, both the dielectric constant and conductivity of tissues on the human back are reconstructed using Micro-GA (MGA) combined with $(\mathrm{FD})^2\mathrm{TD}$. The reconstruction results are compared with references.

2. DESIGN AND OPTIMIZATION OF THE PROBE

There are several kinds of probes and applicators have been investigated, such as antenna arrays [5, 10], waveguides or horns [11], and open-ended coaxial probes [12]. However, in order to simulate the actual tissues using layered-homogenous-tissue model, a suitable probe whose irradiated fields can both penetrate into deeper layers and concentrate in tissues is needed. Moreover, the probe must be used in a wide range of frequencies so that sufficient information can be received in one measurement. Consequently, a patch antenna probe fed by a coaxial line is presented to meet above requirements.

The structure of such a probe is shown in Figure 1, in which cross section is depicted in Figure 1(a), and the circle patch is depicted in Figure 1(b). The inner conductor of the coaxial line is extended to connect with the circle patch. However, the radium of extended inner

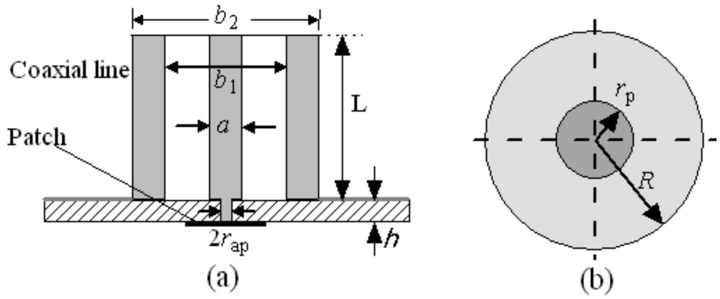

Figure 1. The structure of the patch probe fed by coaxial line (a) Cross section (b) Top view.

conductor r_{ap}, the radium of circle patch r_p, and the thickness of the substrate h need to be optimized to get high performance.

2.1. FDTD Analysis

Finite difference time-domain (FDTD) method is used to calculate the reflection coefficient of the probe and electric field distribution in the tissues, when the probe contacts with tissues directly. The thickness of skin and fat is 0.5 mm and 3.0 mm respectively. And muscle is considered as semi-infinite space. Mur's second order absorbing boundary conditions (ABC) are employed to terminate FDTD computation domain at the planes shown in Figure 2.

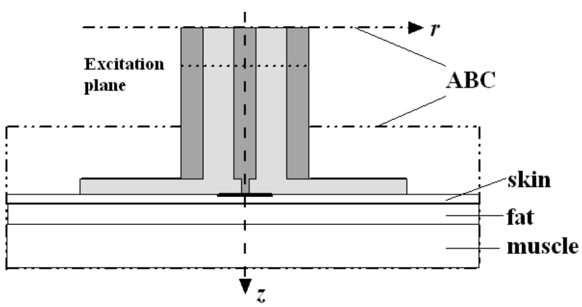

Figure 2. Numerical model.

The FDTD analysis is carried out in a 2-dimensional (2D) cylindrical coordinate since the structure of the probe is rotationally symmetric. The cell size is $\Delta r = \Delta z = \delta = 0.5$ mm, resulting in the time step $\Delta t = 8.3 \times 10^{-13}$ s, and the calculation domain contains 80 $\times$ 220 cells.

The dielectric properties of tissues are obtained from a 4-order Cole-Cole expression [13]:

$$\varepsilon(\omega) = \varepsilon_\infty + \sum_{m=1}^{4} \frac{\Delta\varepsilon_m}{1 + (j\omega\tau_m)^{(1-\alpha_m)}} + \frac{\sigma_j}{j\omega\varepsilon_0} \tag{1}$$

where ε_∞ is high-frequency dielectric constant of tissue, τ is the relaxation time, ε_0 is the permittivity of free space ($= 8.854 \times 10^{-12}$ F/m), σ is the conductivity of tissue in S/m, $\Delta\varepsilon$ is the difference between static dielectric constant and dielectric constant at high frequency, α_m is an constant, and ω is the angle frequency. The parameters used in above equation for skin, fat and muscle can be found in reference [13].

2.2. Micro-GA Optimization

Micro-GA (MGA) is a small-population, nonmutation-based GA that starts with a random and small population size, typically 5~50. The small population size makes it prone to premature convergence to local extrema, thus necessitating the use of the population-restart strategy, in which a new random population is chosen, and the evolution process is restarted by keeping the best individual from the previously converged generations.

The fields irradiated from the probe are expected to penetrate into deeper tissues. And the reflection coefficients at different frequencies are expected to be small so that most of electromagnetic energy can penetrate into tissues. Consequently, the fitness function is defined to be:

$$F = \exp\left(-\alpha_1 \left(\frac{\sum_{i=1}^{n} |S_{11}|_i}{n}\right)^2 - \alpha_2 \left(\frac{\sum_{i=1}^{n} (1/d_i)}{n}\right)^2\right) \tag{2}$$

where α_1, α_2 are constants and $\alpha_1 = \alpha_2 = 10$, $|S_{11}|$ is reflection coefficient of the probe, d is the probing depth, which is defined here by the distance at which the power flowing through the cross section attenuates to 20 dB compared to incident power. And $n = 11$, is the number of frequency points, which are chosen every 0.5 GHz at the frequency range from 2 GHz to 7 GHz.

Here a population size of 5 and uniform crossover with a probability of 0.5 are used in MGA process. The dimensions of the probe are $a = 3.0$ mm, $b_1 = 10.0$ mm, $b_2 = 16.0$ mm and $L = 60$ mm respectively. As a result, optimal parameters are found to be: $r_{ap} = 0.5\,\mathrm{mm}$, $h = 2.5\,\mathrm{mm}$, and $r_p = 2.5\,\mathrm{mm}$.

Experiments are performed to validate both the FDTD calculation and probe optimization. The probing depths of optimized circle patch and of open-ended coaxial line in 1% saline solution at 3 GHz are measured, and results are compared with FDTD simulation. In the experiment, an aluminum plate is put into the saline solution which is filled in a 2-litter beaker and kept at 25°C. The probing depth d is determined by the distance at which the reflection coefficient becomes constant when the plate is moved gradually away from the probe surface in the saline solution [14].

The relative dielectric constant of 1% saline solution is 70.44, and conductivity is 3.461 S/m at temperature 25°C [15]. The plots shown in Figure 3 indicate that the simulation results are in agreement with experimental results. And the probing depth of the optimized circle patch is about 23 mm, which is much deeper than that of open-ended coaxial line, 10 mm. That implies the circle patch can bring more information about deeper tissues, which is very important to the reconstruction of dielectric properties of deeper tissues.

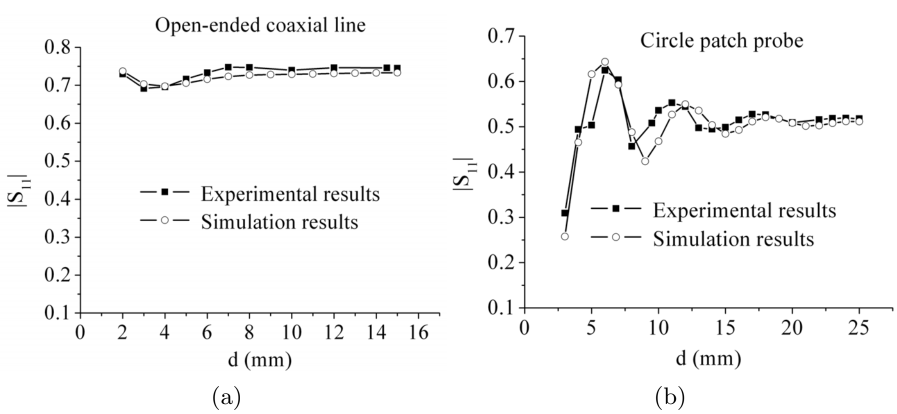

Figure 3. The simulation results of probing depth compared with the experimental results (a) Open-ended coaxial line (b) Circle patch probe.

3. RECONSTRUCTION METHOD

3.1. Debye-model of Tissues

In this section, the method used to reconstruct the dielectric properties of tissues is presented. If the 4-order Cole-Cole model is used to describe the dielectric properties of tissues, 14 parameters need to be reconstructed for each tissue leading to total 44 parameters have to be reconstructed in order to provide the dielectric properties of three kinds of tissues. That is not easy to do. Moreover, the forward problem must be solved using FDTD at each frequency point in that Frequency-dependent FDTD ($(\mathrm{FD})^2\mathrm{TD}$) is hard to perform if the 4-order Cole-Cole model is applied, which will decrease the reconstruction efficiency greatly.

However, if a one-order Debye-model is used, not only the total number of parameters required to describe the dielectric properties decreases to 14, but also $(\mathrm{FD})^2\mathrm{TD}$ can be used to solve the forward problem so that the reflection coefficient at a certain frequency range will be calculated in one computation. As a result, the reconstruction efficiency will be increased greatly. Therefore, a Debye-model is studied to depict the dielectric properties of each tissue at the frequency range from 1 GHz to 7 GHz. The Debye-model is expressed as following:

$$\varepsilon_r = \varepsilon_\infty + \frac{\varepsilon_s - \varepsilon_\infty}{1 + j\omega\tau} + \frac{\sigma}{j\omega\varepsilon_0} \tag{3}$$

where ε_s is the static dielectric constant of tissue, and other parameters have the same meaning as in equation (1). Each parameter is fitted nonlinearly according to the data derived from the 4-order Cole-Cole model, and the results are listed in Table 1.

Table 1. Parameters in Debye-model.

Tissue	ε_s	ε_∞	τ ($\times 10^{-11}$s)	σ (S/m)
Skin	40.6	23.6	1.7	1.0
Fat	5.5	3.4	1.5	0.01
Muscle	53.6	4.3	0.9	1.0

3.2. Reconstruction Method

The inverse problem is solved by a stochastic approach based on a genetic algorithm (GA), which has been applied in some electromagnetic imaging applications, such as MI and EIT [16, 17]. Again the micro-GA is used, but the population size here is 30, much larger than that in probe optimization. Furthermore, a niching technique, sharing is applied to keep the diversity in the population and the niche radius is 0.1. The total generation is set to be 200 to get better results. And the fitness function is defined as:

$$\text{Fitness} = \exp\left[-\alpha \cdot \left(\sum_{i=1}^{n} \left(|S_{11}|_{mea} - |S_{11}|_{cal}\right)^2\right)\right] \tag{4}$$

where α is constant and set to be 0.5. $|S_{11}|_{mea}$ and $|S_{11}|_{cal}$ are reflection coefficients obtained from measurement and FDTD calculation respectively.

3.3. Numerical and Experimental Results

In order to validate the feasibility of the reconstruction algorithm, a numerical simulation of layered tissues is performed first, and then an experiment with layered materials is operated.

Firstly, the forward problem is solved based on Debye-model using $(\text{FD})^2\text{TD}$. Then the results are used as the measured data to reconstruct the dielectric properties of skin, fat and muscle, after they are added randomly 10% error. The thickness of skin and fat are 0.5 mm and 3 mm respectively, and the cell size and time step are the same as that in probe optimization. The excitation used in $(\text{FD})^2\text{TD}$ is modulated Gaussian pulse:

$$E_i(t) = -\cos(\omega t)\exp\left[-\frac{4\pi(t-t_0)^2}{\Delta\tau^2}\right] \tag{5}$$

where t is the present time, t_0 is the time at which the pulse reaches its maximum value, $\Delta\tau$ is time interval. The central frequency is 3.5 GHz, and the total computation time is 10000 time steps. The MGA parameters search spaces for dielectric properties are set broaden enough so that even those that are beyond the values of normal tissues can be detected.

Some preliminary knowledge can be added to provide several restrictions for parameters. For this problem, the known are listed as followings:

a. For each tissue, $\varepsilon_\infty < \varepsilon_s$;
b. For normal tissues, the dielectric constant and conductivity should be smaller than those of skin and muscle.

Putting the known information into the program, some individuals will be eliminated directly without calculating fitness. The reconstructed results are shown in Table 2, where the relative error is defined as:

$$\text{relative error} = \frac{|\text{Reconstruction result} - \text{Original value}|}{\text{Original value}} \times 100\%$$

Results in Table 2 show that an agreement is observed from comparison for most parameters, which validates the accuracy of the reconstruction algorithm of the inverse calculation. But the errors for σ-skin and τ-muscle are large. For σ-skin, the reason is that its value is very small compared to the effective conductivity caused by imagine part of permittivity. For τ-muscle, because muscle is the third layer, the changes of dielectric properties of muscle due to small variation of τ do not influence the reflection coefficient greatly.

Experiments are also performed to examine the validation of the reconstruction algorithm. A flat plate of Teflon is put into pure water to compose a three-layered structure: pure water + Teflon + pure water. The patch probe is connected with Agilent E8362B Vector Network Analyzer and then put into the pure water but apart a certain distant from the Teflon plate. Both the reflection coefficient at the frequency range from 1G Hz to 10 GHz and the distance between probe and Teflon plate are measured. The reconstructed results as well as true values for each parameter are shown in Table 3. The dielectric properties of pure water are described using Debye-model, and keeps constant for Teflon plate.

A good agreement is observed from the comparison except for dielectric constant of Teflon. Because electromagnetic power dissipated much in pure water, which results in a little reflection information from Teflon plate. In summary, both numerical and practical experiments verify the feasibility of applying reconstruction algorithm based on MGA to obtain dielectric properties of lossy dielectric.

4. RECONSTRUCTION OF HUMAN BACK

Using the optimized probe and the reconstruction method mentioned above, the dielectric properties of skin, fat and muscle on a human back, as well as the thickness of skin and fat, are reconstructed.

4.1. Measurement Results

Eight volunteers who have the similar stature and shape are chosen as the sample. For each sample, the backbone is chosen as the axis, and measurement points are marked every 1.5cm along horizontal

Table 2. Reconstruction results.

Parameter	Original value	Reconstruction results	Relative error
ε_s-skin	40.6	40.98	0.009%
ε_∞-skin	23.6	24.7	4 .67%
$\tau\,(\times 10^{-11})$-skin (s)	1.7	1.47	-13.5%
σ-skin (S/m)	1.0	0.7	-30.0%
ε_s-fat	5.5	4.82	-14.1%
ε_∞- fat	3.4	2.67	-21.5%
$\tau\,(\times 10^{-11})$- fat(s)	1.5	1.47	-2.00%
σ- fat(S/m)	0.01	0.0098	-2.00%
ε_s -muscle	53.6	54.05	0.84%
ε_∞- muscle	4.3	4.16	-3.25%
$\tau\,(\times 10^{-11})$- muscle (s)	0.9	1.12	24.4%
σ- muscle (S/m)	1.0	0.85	9.4%
Thickness of skin (mm)	0.5	0.5	0
Thickness of fat (mm)	3.0	2.5	-16.7%

Table 3. Reconstructed results in comparison with true value for pure water and teflon.

Parameter		True value	Reconstructed results	Relative error
Pure water	ε_s	80.0	76.1	-4.86%
	ε_∞	1.8	1.80	0 .0%
	$\tau\ (\times 10^{-12})$	9.4	9.96	5.96%
	σ_1	0.0	0.0097	----
Teflon	ε_r	2.06	2.85	38.6%
	σ_2	0.0005	0.006	----

line and every 2cm along vertical line on both sides of the backbone. Consequently total 460 points need to be measured for each sample.

An Agilent E8362B Vector Network Analyzer is used to measure the reflection coefficient of the patch probe which is kept contact with skin tightly. Measurement results at 801 frequency points ranging from 1 GHz to 7 GHz are restored for each measurement point. The measured results from 2 GHz to 7 GHz are shown in Fig. 4.

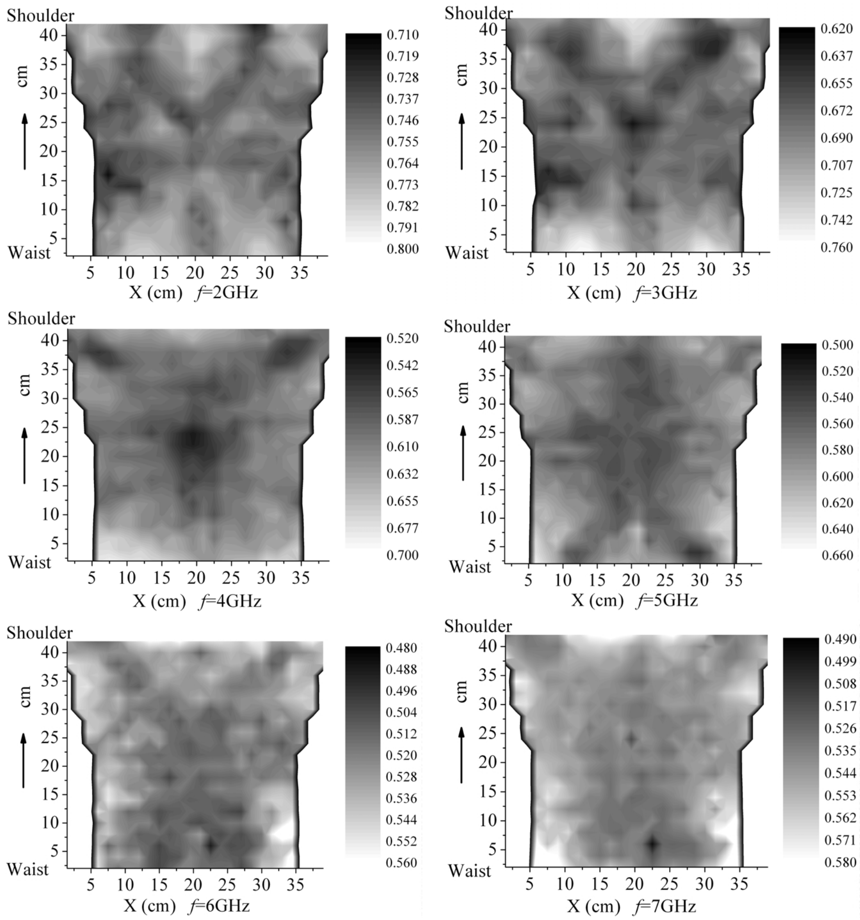

Figure 4. The reflection coefficient measured at different position on the human back at different frequency points.

In Figure 4, backbone locates at $x = 20\,\text{cm}$, while waist at 0cm and shoulder at 42 cm along vertical axis. The results indicate that the reflection coefficient $|S_{11}|$ decrease gradually as frequency increases. At the same frequency, $|S_{11}|$ varies greatly in terms of position on human back. It is smaller in the area with more bones (such as backbone and bladebone) than that in the area with more fat (such as waist), especially at the frequency 2∼5 GHz. That implies the field irradiated from the probe can penetrate tissues deeply, as shown in Figure 3. Moreover, the distribution of $|S_{11}|$ is in good agreement with the symmetric structure of human back.

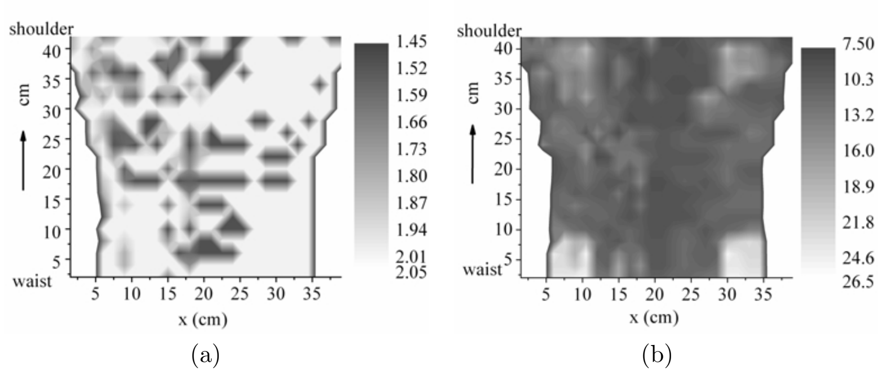

Figure 5. Reconstructed thickness of skin and fat (a) Thickness of skin, (b) Thickness of fat.

4.2. Reconstructed Results

Using the experimental results and reconstruction method mentioned above, the dielectric properties of skin, fat and muscle are reconstructed, as well as thickness of skin and fat (see Figure 5).

It can be found in Figure 5(a) that the thickness of skin varies from 1.5 mm to 2 mm. Moreover the thickness of skin on most part of the back is approximately 2 mm, which is in good agreement with the reference [18]. However, the thickness of fat varies greatly on the back, from 8.0 mm to 26 mm, especially the fat is much thicker around the waist than along the backbone. The sample is 172 cm high and weighs 63 kg. Therefore, the reconstructed results of fat are in accordance with the fact of the sample.

Figures 6(a) and (b) show the reconstructed dielectric properties of skin at 3 GHz. The dielectric constant varies between 35.5 and 41.3, and the conductivity varies between 1.65~2.21, while the values derived from the 4-order Cole-Cole model are 39.0 and 1.85 respectively. The maximum relative error is 9.0% for reconstructed dielectric constant and 19% for conductivity when compared to the values from the 4-order Cole-Cole model.

The reconstructed dielectric properties of fat are shown in Figures 7(a) and (b). The maximum relative error is 14% for dielectric constant and 27% for conductivity in comparison with the values 5.3 and 0.11, obtained from the 4-order Cole-Cole model. The maximum error of conductivity is large because the conductivity of fat is very small and the fat is on the second layer.

As for the muscle, the reconstructed results are shown in Figures 8(a) and (b). The dielectric constant of muscle is between

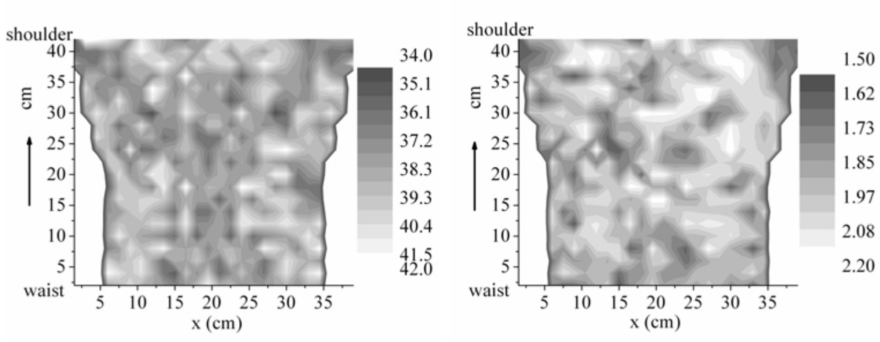

(a) (b)

Figure 6. Reconstructed dielectric properties of skin at 3 GHz (a) Dielectric constant, (b) Conductivity.

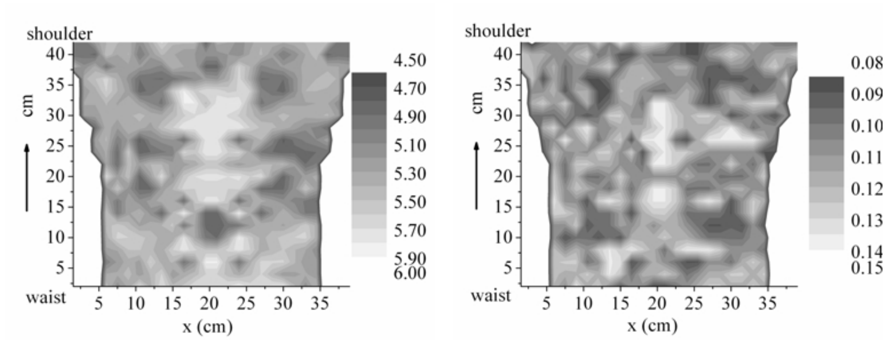

(a) (b)

Figure 7. Reconstructed dielectric properties of fat at 3 GHz (a) Dielectric constant, (b) Conductivity.

46.0∼53.6 with the maximum error 12% compared to 52.2 (4-order Cole-Cole model). And the conductivity is between 2.10∼2.72 with the maximum error 16% compared to 2.35 (4-order Cole-Cole model).

In a summary, most of reconstructed results are close to the values derived from the 4-order Cole-Cole model, though the maximum relative error is large at a few points on the human back. These errors may be decreased by both improving the reconstruction method and redesigning the patch probe.

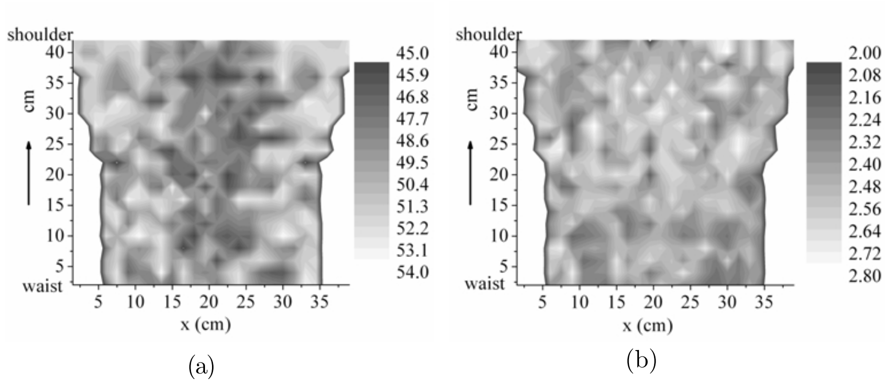

Figure 8. Reconstructed dielectric properties of muscle at 3 GHz (a) Dielectric constant, (b) Conductivity.

5. CONCLUSIONS

A noninvasive method to determine the dielectric properties of layered tissues is presented. A circle patch probe fed by coaxial line is optimized using MGA in order to not only let the layered-homogenous-tissue model suitable for the actual biological tissues but to measure reflection coefficients in a wide frequency range. Then a MGA inverse computational scheme is applied to reconstruct the tissue's dielectric properties. Both numerical simulation and experiment are employed to investigate the feasibility of this method. The reconstructed results of layered material composed of pure water and Teflon plate are compared with its true value. An agreement is observed from the comparison, which validates the feasibility of the proposed method.

Finally, the optimized probe and proposed method are used to reconstruct the dielectric properties of skin, fat and muscle, as well as thickness of skin and fat on the human back. And the reconstruction results are in a good agreement with the value derived from 4-order Cole-Cole model. The future work is to improve the precise of reconstructed results by redesigning the patch probe and modifying the MGA scheme.

ACKNOWLEDGMENT

This project was supported by National Science Fund of China.

REFERENCES

1. Fear, E. C., S. C. Hagness, P. M. Meaney, M. Okoniewski, and M. A. Stuchly, "Enhancing breast tumor detection with near-field imaging," *IEEE Microwave Magazine*, 48–56, Mar. 2002.
2. Chaudhary, S. S., R. K. Mishra, A. Swarup, and J. M. Thomas, "Dielectric properties of normal and malignant human breast tissues at radiowave and microwave frequencies," *Indian J. Biochem., Biophys.*, Vol. 21 76–79, Feb. 1984.
3. Joines, W. T., Y. Z. Dhenxing, and R. L. Jirtle, "The measured electrical properties of normal and malignant human tissues from 50 to 900 MHz," *Med. Phys.*, Vol. 21, 547–550, Apr. 1994.
4. Rius, J. M., C. Pichot, L. Jofre, et al., "Planar and cylindrical active microwave temperature imaging: numerical simulation," *IEEE Trans. Med. Imag.*, Vol. 11, 457–469, Apr. 1992.
5. Fear, E. C., Xu Li, S. C. Hagness, and M. A. Stuchly, "Confocal microwave imaging for breast cancer detection: localization of tumors in three dimensions," *IEEE Trans. Biomed. Eng.*, Vol. 49, 812–822, Oct. 2002.
6. Bond, E. J., Xu Li, S. C. Hagness, and B. D. Van Veen, "Microwave imaging via space-time beamforming for early detection of breast cancer," *IEEE Trans. AP*, Vol. 51, 1690–1705, Oct. 2003.
7. Vauhkonen, P. J., et al., "Three-dimensional electrical impedance tomography based on the complete electrode model," *IEEE Trans. Biomed.*, Vol. 46, 1150-1-160, Sep. 1999.
8. Huang, K., X.-B. Xu, and L.-P. Yan, "A new noninvasive method for determining the conductivity of tissue embedded in multilayer biological structure," *J. of Electomagn. Waves and Appl.*, Vol. 16, 851–860, Jun. 2002.
9. Klemm, M. and G. Troester, "EM energy absorption in the human body tissues due to UWB antennas," *Progress In Electromagnetics Research*, PIER 62, 261–280, 2006.
10. Gupta, R. C. and S. P. Singh, "Elliptically bent slotted waveguide conformal focused array for hyperthermia treatment of tumors in curved region of human body," *Progress In Electromagnetics Research*, PIER 62, 107–125, 2006.
11. Gupta, R. C. and S. P. Singh, "Development and analysis of a microwave direct contact water-loaded box-horn applicator for therapeutic heating of bio-medium," *Progress In Electromagnetics Research*, PIER 62, 217–235, 2006.

12. Huang, R. F. and D. M. Zhang, "Application of mode matching method to analysis of axisymmetric coaxial discontinuity structures used in permeability and/or permittivity measurement," *Progress In Electromagnetics Research*, PIER 67, 205–230, 2007.
13. Gabriel, C. and S. Gabriel, "Compilation of the dielectric properties of body tissues at RF and microwave frequencies," Physics Department, King's College London, London WC2R 2LS, UK. Legal Documentation from http://www.brooks.af.mil/AFRL/HED/hedr/reports/dielectric
14. Hoshina, S., Y. Kanai, and M. Miyakawa, "A numerical study on the measurement region of an open-ended coaxial probe used for complex permittivity measurement," *IEEE trans. Mag.*, Vol. 37, 3311–3314, May 2001.
15. Stogryn, A., "Equations for calculating the dielectric constant of saline water," *IEEE, Trans. MTT*, Vol. 19, 733–736, Oct. 1971.
16. Chiu, C.-C. and W.-T. Chen, "Electromagnetic imaging for an imperfectly conducting cylinder by the genetic algorithm," *IEEE Trans. MTT.*, Vol. 48, 1901–1905, Nov. 2000.
17. Caorsi, S. and M. Pastorino, "Two-dimensional microwave imaging approach based on genetic algorithm," *IEEE trans. AP.*, Vol. 48, 370–373, Mar. 2000.
18. Zheng, R. Q., S. W. Zhang, H. J. Lin, et al., "Study of normal human skin with 15 MHz ultrasound," *China Journal of Ultrasonography*, Vol. 16, 85–87, Mar. 1997.